BIOMASS AND BIOENERGY 62 (2014) 149–157

Available online at www.sciencedirect.com

ScienceDirect

http://www.elsevier.com/locate/biombioe

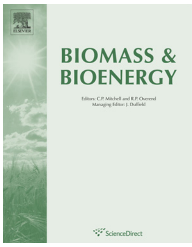

Effect of pyrolysis temperature on miscanthus (*Miscanthus* × *giganteus*) biochar physical, chemical and functional properties

T. Mimmo [a], P. Panzacchi [b,c,*], M. Baratieri [a], C.A. Davies [b], G. Tonon [a]

[a] Faculty of Science and Technology, Free University of Bolzano, Piazza Universitá 5, Bolzano, Italy
[b] Shell International Exploration and Production Inc., Shell Technology Centre Houston, P.O. Box 4685, Houston, TX 77251, USA
[c] Department of Agricultural Sciences-DipSA, Viale Fanin, 46, 40127 Bologna, Italy

ARTICLE INFO

Article history:
Received 22 July 2013
Received in revised form
3 January 2014
Accepted 6 January 2014
Available online 28 January 2014

Keywords:
Miscanthus
Biochar
Characterization
Pyrolysis temperature
Biochar stability
Carbon sequestration

ABSTRACT

The thermal conversion (pyrolysis) of biomass for energy production and the incorporation into agricultural soils of the carbon-rich byproduct (biochar) can contribute to the mitigation of climate change. The beneficial effect of biochar on soil fertility and its stability to degradation depends on the interactions of soil and climatic conditions with biochar physicochemical properties, the latter mainly depend on feedstock and pyrolysis conditions. The aim of the present research was to study the effect of pyrolysis temperature on physicochemical properties of miscanthus (*Miscanthus* × *giganteus*) biochar and on its short-term stability. Biochar properties were assessed by FTIR spectroscopy, CHN-elemental and simultaneous thermogravimetry (STA) analyses and the short-term stability in a 6-month incubation experiment. All the analytical techniques indicated a threshold value of pyrolysis temperature of 360 °C, above which the thermal and biological resistance to degradation increased dramatically. FTIR spectroscopy showed characteristic absorption bands of cellulose and hemicelluloses (1000–1200 cm^{-1}) in the low-temperature biochars that disappeared in high-temperature biochars. In these latter the absorption peaks associated with aromatic structures increased as confirmed by the decrease of both O/C and H/C ratios. This finding agrees with the STA results showing an increase of DTG temperature peak for high pyrolysis temperatures biochars. The incubation experiment confirmed an increased resistance to biological decomposition of biochar produced at temperatures above 360 °C. The results of the present study demonstrate that biochar thermal and biological stability is affected by pyrolysis temperature in a nonlinear manner.

© 2014 Elsevier Ltd. All rights reserved.

1. Introduction

Producing energy from renewable sources and improving environmental sustainability by reducing nutrient leaching, greenhouse gas (GHG) emissions, sequestering carbon (C) and increasing soil fertility are key points of the current European agro-ecological policy [1]. The thermal conversion of plant biomass and the incorporation into agricultural soils of its C-

---

[*] *Corresponding author*. Department of Agricultural Sciences-DipSA, University of Bologna, Viale Fanin, 46, 40127 Bologna, Italy. Tel.: +39 (0)512096460; fax: +39 (0)512096401.
E-mail address: pietro.panzacchi@unibo.it (P. Panzacchi).

0961-9534/$ – see front matter © 2014 Elsevier Ltd. All rights reserved.
http://dx.doi.org/10.1016/j.biombioe.2014.01.004

rich by-product, biochar, can contribute to achieving these ambitious goals [2–5]. In temperate climates, miscanthus (*Miscanthus* × *giganteus*) is one of the most promising energy crops, as it is a fast-growing species with low nutrient requirements and high yields [6,7]. Miscanthus has been proven to be a valuable crop for co-firing with coal to produce power and reduce CO_2 emissions [8–10]. However, thermo-chemical conversion processes, such as pyrolysis, are proposed to be a more efficient multipurpose technology than combustion to produce power, heat and sequester carbon, especially when biochar is used as a soil amendment [11,12]. Recently, biochar obtained from miscanthus has been studied either because its increasing availability as a feedstock for second generation biofuels [13,14] or for its natural enrichment in ^{13}C which make it a useful tool to study the fate of the biochar C after biochar application to the soil [15] or its effect (priming) on soil organic matter (SOM) [16].

Due to contrasting results, the effect of biochar on soil properties and crop productivity as well as the stability of biochar to microbial decomposition is still under debate [17]. A recent meta-analysis of the biochar effect on plant productivity, based on 103 published studies, found that biochar soil amendment increased crop productivity by 11% on average, although large differences among studies have been observed depending on experimental conditions [18]. Similarly, the effect of biochar on nutrient leaching and immobilization was found to depend on biochar characteristics, soil properties and climatic conditions [19–21]. For example, Kameyama et al. [22], studying the effect of biochar on nitrate (NO_3^-) leaching found that NO_3^- was weakly sorbed to biochar surfaces, but sorption increased with pyrolysis temperatures due to the formation of base functional groups. Also the short-term stability of biochar was found to depend on feedstock, temperature of pyrolysis and application rate [23–26]. The pyrolysis temperature seems to affect also the interaction of biochar with the biogeochemical processes that drive the GHG production. For example, Ameloot et al. [27] found that biochar produced at high pyrolysis temperatures reduced the cumulative (biochar- + SOM-derived) CO_2 and N_2O fluxes more than biochars produced at low temperatures. The beneficial effect of biochar on soil fertility and its stability to degradation seem to be highly dependent on the interactions of biochar physicochemical properties with soil and climatic conditions. In this context, feedstock properties and pyrolysis conditions such as temperature and residence time are the major contributing factors to the physicochemical characteristics of biochar [28]. Different feedstocks differ in both elemental composition and content of cellulose, lignin, hemicelluloses, waxes, etc., all of which influence the chemical and physical structure of the biochar [29,30]. Depending on pyrolysis temperature, biomass feedstock undergoes several chemical and physical changes. Among them, changes in C/N, O/C, and H/C ratios, cation exchange capacity (CEC), porosity, increase in aromatic carbon–carbon double bonds (C=C) and a decrease in O–H and CH_3 have frequently been reported in the literature [31–34]. Specifically, the pyrolysis occurs via a series of complex reactions that can be divided into stages according to the temperature of degradation for the hemicelluloses (220–315 °C), cellulose (315–400 °C) and lignin (>400 °C) [35]. As a consequence, it is a key point to characterise biochars produced at different pyrolysis temperature with appropriate analytical techniques in order to get information on the biochar chemical structure and physical characteristics that can be associated with biochar stability and agronomic benefits.

The aims of this research are: i) to investigate by means of simultaneous thermogravimetric analysis (STA) and Fourier transform infrared (FTIR) spectrometry the physicochemical properties of five different miscanthus biochars produced between 350 and 450 °C, ii) to assess the short-term stability of these biochars by measuring the mineralization rates in a six-month incubation experiment, iii) to assess the relationship between the biochar physicochemical properties and the short-term stability in soil conditions.

2. Materials and methods

2.1. Biochar production

Biochar was produced by the Biomass Technology Group (BTG) B.V. (Enschede, NL) from miscanthus cultivated in the Groningen province, Netherlands (53°13′00″ N, 6°34′00″ E), and chipped to ~20–40 mm prior to pyrolysis. The pyrolysis unit used by BTG consists of a screw reactor indirectly heated by means of the hot gas derived from a combustor. The biomass (average moisture and ash mass fraction of 11% and 2.3%, respectively), was manually fed into an initial screw reactor and subjected to temperatures around 120–130 °C to reduce the moisture content. After passing through the initial screw reactor, the biomass was then pyrolysed in a second screw reactor at different pyrolysis temperatures (350, 360, 370, 400 & 450 °C). Both reactors consist of two concentric tubes, the inner tube holds a conveyor while the outer shell acts as the heating jacket. The reactors are heated by the combustion of vapours and gasses originating from the pyrolysis process and conveyed to a combustor in which they are mixed with air and combusted at an operating temperature of 850 °C. The residence times in the second screw reactor at pyrolysis temperatures averaged 14.7 ± 0.4 min and biochar yields (expressed as mass fraction of the original wet biomass) varied between 31% and 73% for 450 and 360 °C, respectively (Table 1).

2.2. Elemental analysis of biochars and soil

Carbon (C), nitrogen (N) and hydrogen (H) content of biochars, feedstock and soil were determined by dynamic flash combustion using a Thermo Flash 2000 elemental analyzer (Thermo Fisher Scientific Inc., USA). Oxygen (O) content was calculated by difference (100% –C, H,N, O, ash %). The elemental analyzer (EA) was configured with a pre-packed oxidation and reduction column consisting of chromium oxide and silvered cobaltous/ic oxide (OEA Labs Ltd, United Kingdom). The system gas flow rates were, He carrier gas (flow rate 100 mL min^{-1}), reference gas flow rate (250 mL min^{-1}), O_2 injection of 5 s (flow rate 240 mL min^{-1}) and a 12-s sample delay. Prior to analysis samples were oven dried at 105 °C, ball milled and weighed (~2 mg) in triplicate into tin capsules. Samples were then run using the system described above with

Table 1 – Residence time, yield (% of the original wet biomass remaining after pyrolysis), elemental composition (ash free), pH and field capacity (FC) of miscanthus, biochar and soil samples ($n = 3$, mean ± standard deviation for CNH composition, pH and FC).

	Residence time (min)	Yield (%)	N (%)	C (%)	H (%)	O (%)	pH	FC (g kg^{-1})
Miscanthus	–	–	0.31 ± 0.01	46.34 ± 0.14	5.88 ± 0.03	47.62	6.36 ± 0.07	309.9 ± 13.3
Biochar 350 °C	15.1	70	0.30 ± 0.03	50.95 ± 0.20	5.76 ± 0.61	43.14	6.90 ± 0.02	236.9 ± 11.1
Biochar 360 °C	14.8	73	0.32 ± 0.02	51.83 ± 0.35	5.91 ± 0.27	42.09	7.17 ± 0.01	207.3 ± 2.5
Biochar 370 °C	14.0	40	0.58 ± 0.10	68.16 ± 0.37	5.05 ± 0.92	26.46	8.63 ± 0.04	290.0 ± 15.3
Biochar 400 °C	15.1	37	0.64 ± 0.00	69.84 ± 0.39	4.65 ± 0.00	25.11	8.83 ± 0.01	486.6 ± 15.1
Biochar 450 °C	14.3	31	0.56 ± 0.01	72.61 ± 0.76	4.21 ± 0.06	22.91	9.25 ± 0.01	450.7 ± 17.2
Soil	–	–	0.12 ± 0.03	1.87 ± 0.16	0.53 ± 0.03	47.62	5.10 ± 0.02	71.7 ± 0.2

certified reference samples with similar C/N ratios every 15 experimental samples.

2.3. *Field capacity and pH of biochars*

The biochar and soil pH were determined by mixing soil or biochar with de-ionized (DI) water (ratio of 1:1 by weight), the sample was then left to stand for 10 min before measuring the pH with a pH meter (Mettler-Toledo, USA).

The soil and biochar field capacity (FC) was determined gravimetrically as the amount of water held after saturation and subsequent free drainage of water from the samples. The soil and biochar were placed in a folded Whatman 42 filter paper placed in funnel that was suspended over a conical flask. The samples were then fully saturated with water and allowed to drain for 2 h. Biochar samples were shaken with DI water for 2 h to allow the pores to become fully saturated before drainage. Field capacity was then determined as mass of water retained per mass of dry soil or biochar.

2.4. *Thermal analysis*

Thermal analysis (thermogravimetric/TG) and derivative (DTG) profiles of dried and ball milled feedstock and biochar obtained at 350, 360, 370, 400 and 450 °C were obtained using a simultaneous thermogravimetric analyser (STA 449 F3, Netzsch, Germany) at the applied laboratory of NETZSCH-Gerätebau in Selb, Germany. STA analyses were performed under inert helium atmosphere at a constant heating rate of 10 K min^{-1} in a temperature range from ambient temperature to 1000 °C.

2.5. *FTIR spectroscopy*

The FTIR spectra of the miscanthus feedstock and the biochar samples obtained at 350, 360, 370, 400 and 450 °C were recorded on a Bruker Tensor 27 spectrophotometer (Bruker, USA). The instrument was fitted with a platinum accessory for attenuated total reflectance (ATR). Samples could thus be analysed without KBr dilution. Spectra were an average of 64 scans at a resolution of 4 cm^{-1}.

2.6. *Biochar incubation in soil*

The biochar incubation assays were performed using soil collected from the plough layer (0–30 cm) of an arable field in a commercial farm near Lincolnshire, England (53°18′190″N, 0°34′040″W). The soil characteristics are reported in Table 1. The soil was air dried and sieved (2 mm), then 10 g of soil and 5 g of biochar or miscanthus biomass were mixed in triplicate in 50 mL tubes (BD Falcon, BD biosciences, USA). Deionized (DI) water was then added to the mixture to achieve 65% of FC. The total weight was recorded so that moisture content could be maintained throughout the 169-day incubation by weighing every two weeks and adding DI water to bring the sample weight back to the original mass. Assay tubes were stored in a ventilated incubator at 10 °C without lids to prevent build-up of CO_2 and reductions of O_2 in the headspace, which would inhibit microbial activity. Tubes were covered with Parafilm perforated to reduce evaporative moisture losses. The soil CO_2 flux was measured 1, 50, 111 and 169 days after the biochar soil addition and expressed as μg of CO_2 per hour per gram of C content of the soil and biochar mixture. For this purpose the tubes were capped with a lid modified with an isobutylene-isoprene rubber septa and an O-ring, flushed with CO_2-free air at 100 kPa pressure for 2 min through two needles inserted in the septa prior to incubation at 10 °C overnight. To sample the headspace air 10 mL of pure N_2 were firstly injected into the sealed tube using a 25 mL gas tight syringe (SGE Analytical Science, Australia). The syringe was flushed three times to allow the adequate mixing of the headspace. Fifteen mL of gas were then pulled back into the syringe, and 10 mL of them were injected into a 12 mL screw capped glass vial (Exetainer, Labco Ltd, United Kingdom) pre-filled with N_2 de-gassed DI water. A second syringe needle inserted just through the septa of the inverted vial allowed the water to be displaced by the 10 mL of headspace gas sample. Then the second syringe needle was removed and the remaining 5 mL of gas sample injected to over pressurize the sample in the vial. The vials were then stored inverted at room temperature and in dark condition until analysis.

To determine the CO_2 concentration 5 mL of the sample gas were injected in the gas chromatograph (GC Agilent 7890A, Agilent Technologies, USA) fitted with a FID with a methaniser in series, TCD and μECD. Samples were injected via a split/splitless injector onto a Poroplot Q capillary column and then split to the three detectors via a microfluidic dean switch. The GC was run isothermally at 40 °C, and the FID, μECD at 300 °C and 350 °C respectively.

2.7. *Data analysis*

The effect of pyrolysis temperature on CO_2 efflux from biochar-treated soil has been analysed as a repeated measures experiment using the General Linear Models (GLM) procedure in SPSS v. 20 software (IBM corporation, USA) with pyrolysis temperature as between-subject factor and time as within-subject repeated factor. The prerequisite of the sphericity of the variables was tested by Mauchly's sphericity test and when the sphericity was not satisfied the Epsilon of Greenhouse – Geiser correction was used. A multiple comparison procedure was then used to analyse statistically differences among means using the Duncan's multiple comparison procedure ($p < 0.05$). The effect of pyrolysis temperature on cumulated CO_2 flux at the end of the incubation was tested by one way ANOVA with Statgraphics Centurion XV software (StatPoint Inc., USA). Differences among the means were tested with the Tukey's honestly significance differences (HSD) procedure.

3. Results

3.1. *Elemental characterization of biochar*

Table 1 shows the main characteristics of the miscanthus feedstock and biochars produced at different temperatures. The biochar yield expressed as percent of the original wet biomass remaining after pyrolysis, decreased with increasing reactor temperature. While the O and H content markedly decreased with increasing pyrolysis temperature, the opposite happened to C and N content. The largest change in biochar elemental composition was observed between pyrolysis temperatures of 360 and 370 °C (Table 1). This can be well represented by the Van Krevelen diagram (Fig. 1), where increasing pyrolysis temperature results in a biochar composition more similar to that of charcoal. The O/C and H/C ratio decreased with increasing pyrolysis temperature, with the greatest changes in the elemental composition occurring between 360 and 370 °C. After this "threshold" value, further increases in pyrolysis temperature produced only slight changes in both H/C and O/C ratio (from 0.88 to 0.69 and from 0.29 to 0.24, respectively) (Fig. 1).

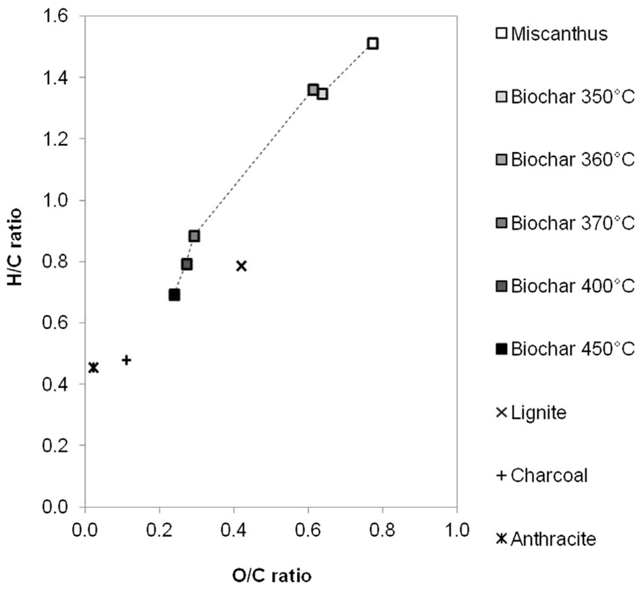

Fig. 1 – Van Krevelen plot of elemental ratios for miscanthus biochars obtained at 350 °C, 360 °C, 370 °C, 400 °C and 450 °C, lignite [51] anthracite [52] and charcoal [53].

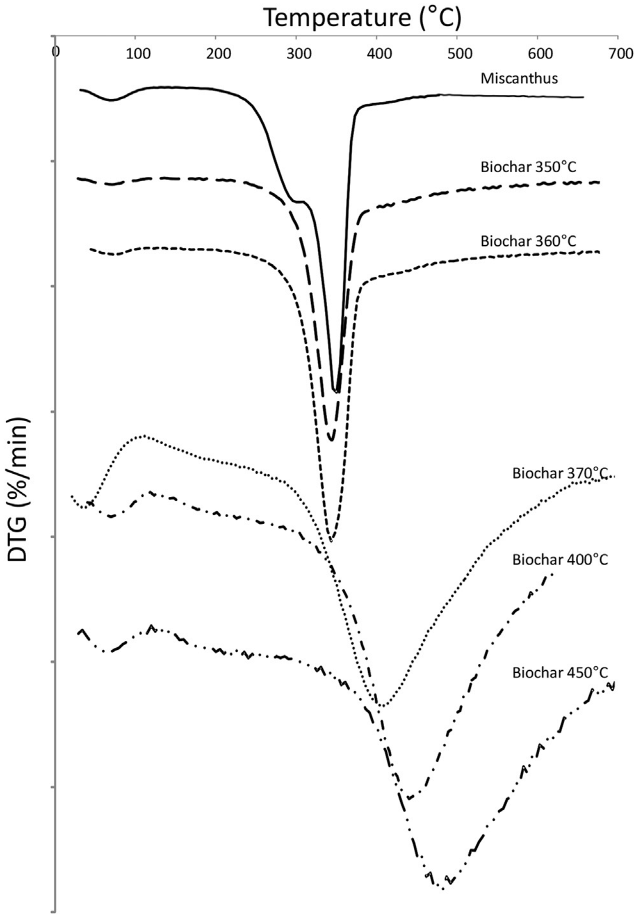

Fig. 2 – DTG profiles of miscanthus and biochar samples obtained at 350 °C, 360 °C, 370 °C, 400 °C and 450 °C (Temperature in function of DTG signal – % min^{-1}).

3.2. *Field capacity and pH*

There was an increase in the biochar pH with increasing pyrolysis temperature from 6.36 to 9.25 for the feedstock and the biochar produced at 450 °C, respectively. The largest increase in biochar pH as function of pyrolysis temperature was observed between 360 °C and 370 °C (Table 1). The FC was lower for biochars produced at 350–370 °C, and higher for biochars produced at 400 °C and 450 °C compared to the feedstock (Table 1).

3.3. *Thermal analysis*

The thermal degradation of the biochar samples occurred in one step, which broadened with increasing pyrolysis temperature as can be observed by the DTG profiles (Fig. 2). The thermal degradation behaviour of biochar produced at 350 and 360 °C was similar to that of the feedstock. The thermal degradation profile of the original feedstock showed a shoulder between 270 and 300 °C, which disappeared in the biochars. In these three cases the thermal degradation started at 250 °C and ended at around 400 °C with a 70% mass loss (Table 2, Fig. 3).

Thermal degradation profiles changed significantly at pyrolysis temperatures greater than 360 °C (Figs. 2 and 3). The degradation reactions occurred over a much broader temperature range between 300 and 600 °C. Generally, the higher the pyrolysis temperature the higher the DTG peak temperature and the residual mass (Table 2).

3.4. *FTIR spectroscopy*

The ATR-FTIR spectra of the miscanthus feedstock and the miscanthus biochar obtained at 350, 360, 370, 400 and 450 °C are shown in Fig. 4. Biochar produced at 350 and 360 °C had spectral features similar to that of the original feedstock (bands between 1200 and 1000 cm^{-1}). Higher pyrolysis temperatures, i.e. 370, 400 and 450 °C induced a broadening and decreasing intensity of the O–H stretching of the hydroxyl groups at 3200–3400 cm^{-1} due to the loss of hydration. In addition, absorption intensities at 1610–1740 cm^{-1} arising from C=O stretching of ketones and other carbonyl structures disappeared in the biochar samples obtained at temperatures >360 °C. Temperatures higher than 360 °C also caused the disappearance of the peak at 1030 cm^{-1} due to C–O and C–O–C stretching, which is characteristic of the anomeric region of cellulose-like structures. Concomitantly, at 370–450 °C, sharp absorption peaks arise at 1590 cm^{-1} due to aromatic C=O and C=C stretching. Higher pyrolysis temperatures (>360 °C) caused also an increase in FTIR signals in the fingerprint region between 700 and 850 cm^{-1} which is characteristic of aryl C–H and/or aryl C–O groups.

3.5. *Biochar incubation in soil*

The CO_2 flux normalized for the C content of the soil/biochar mixture was significantly greater ($p < 0.05$) for the feedstock than for all the other charred materials (Fig. 5a and b). However, the biochars produced at temperatures higher than 370 °C emitted less CO_2 than that of all the other biochars (Fig. 5a and b) ($p < 0.05$), and the CO_2 flux remained almost constant throughout the experimental time (Fig. 5a). By contrast the CO_2 flux of feedstock and biochars produced at temperatures lower than 370 °C showed a peak at the first sampling time (day 1) followed by a sharp decrease at the second sampling time (day 50). The statistical analysis showed that CO_2 fluxes emitted by biochars produced at 350 and 360 °C are significantly different from those of the feedstock and biochars produced at higher temperatures ($p < 0.05$).

Table 2 – Thermogravimetric temperature loss from ambient temperature to 648 °C, peak temperatures of the derivative (DTG) profiles and the residual mass loss at 648 °C for Miscanthus and biochars obtained at 350, 360, 370, 400 and 450 °C.

Sample	TG loss up to 648 °C (%)	DTG peak temperature (°C)	Residual mass at 648 °C (%)
Miscanthus	78.86	369.5	18.05
Biochar 350 °C	64.79	341.1	33.36
Biochar 360 °C	65.30	342.6	32.30
Biochar 370 °C	32.80	405.8	63.70
Biochar 400 °C	25.55	450.1	69.65
Biochar 450 °C	20.51	481.2	73.15

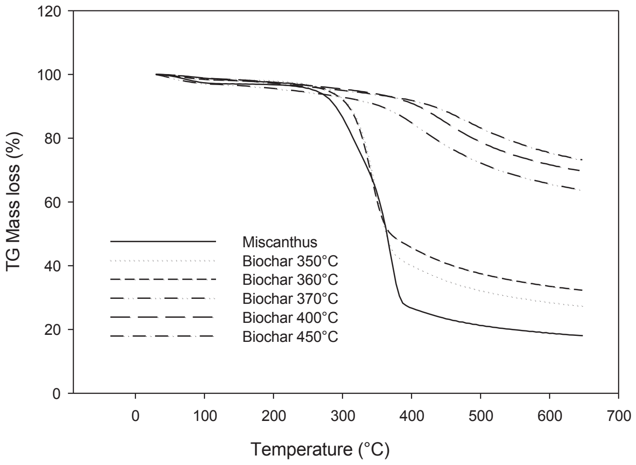

Fig. 3 – Thermogravimetric mass loss in function of temperature for miscanthus and biochar samples obtained at 350 °C, 360 °C, 370 °C, 400 °C and 450 °C.

4. Discussion

4.1. *Biochar basic characterization*

The yield of biochar decreased as expected [36] with increasing the temperature of pyrolysis (Table 1), as a result of a greater thermal decomposition of organic material. However, the biochar yields obtained at 350 °C and 360 °C are higher than those reported for slow pyrolysis from similar feedstock [24,37]. The shorter residence time compared to the above mentioned studies and the moderate severity of the process for the two lower temperatures have likely produced just a partial degradation of cellulose and hemicelluloses as was confirmed by the STA and FTIR analyses (see Sections 3.3 and 3.4).

The FC or water holding capacity of charred plant material has been related to its total pore volume and porosity structure [38,39], which in turn, is controlled by pyrolysis conditions and the chemistry and physical structure of the original biomass feedstock [40]. In this study the FC of biochars produced at 350 °C and 360 °C is lower than that of the original feedstock, increasing for pyrolysis temperature >360 °C (Table 1). Brewer et al. (unpublished data) characterising the porosity of the same set of biochars, found a limited pore connectivity of the two lowest temperatures biochars and postulated a pore occlusion by condensation of volatiles which could explain the lower FC. The observed trend of FC values in relation to pyrolysis temperature >360 °C, agrees with the results published by Kinney et al. [37] for slow pyrolysis biochar produced from corn stover. The authors found an optimal pyrolysis temperature, comprised between 400 and 600 °C for which the porosity and consequently FC reaches a maximum.

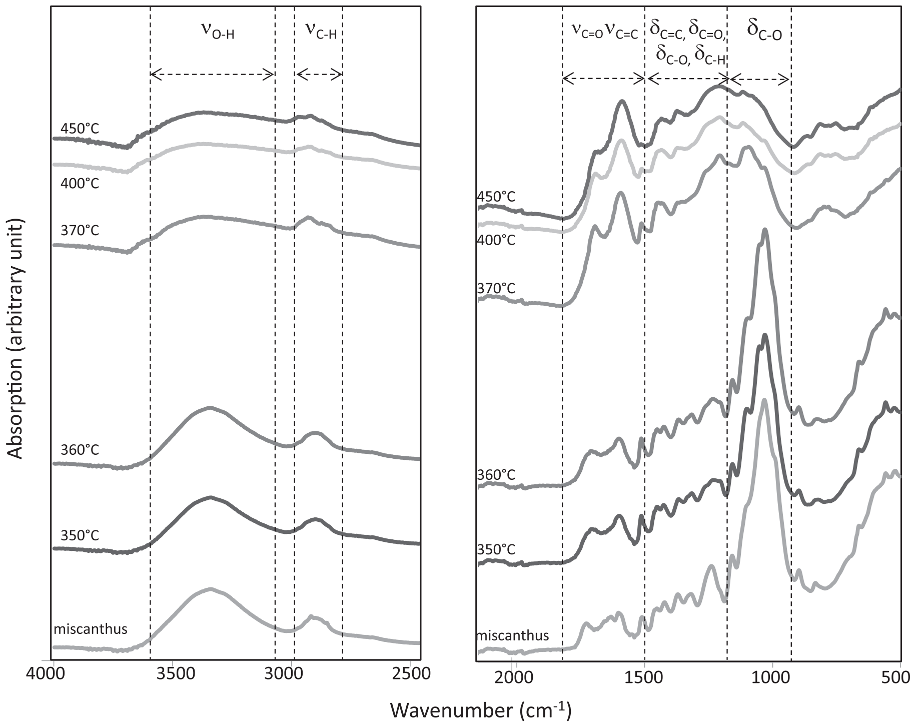

Fig. 4 – Stacked FTIR spectra of miscanthus and biochar samples obtained at 350 °C, 360 °C, 370 °C, 400 °C and 450 °C.

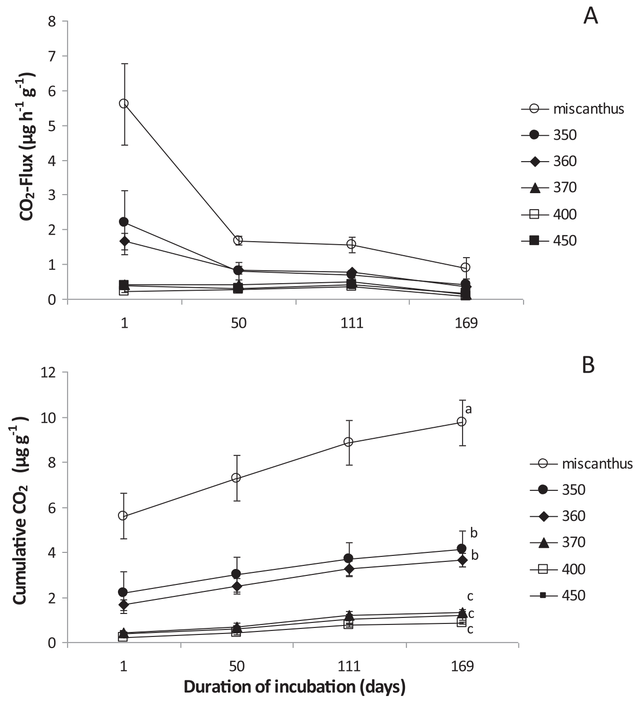

Fig. 5 – A) Measured soil CO_2 efflux based on fixed C content after application of different biochar and miscanthus feedstock. B) Cumulative CO_2 flux based on fixed C content of soil plus biochar and miscanthus feedstock. Values are the mean ($n = 3$) ± S.E. (bars). Different letters indicate statistically different values ($p < 0.05$).

The rise in biochar pH with increasing pyrolysis temperature (Table 1) has been widely reported [17,34,37] and associated with the increase in ash content and oxygen functional groups occurring during the thermo-chemical conversion of the biomass [37]. Schneider et al. [41] observed that pH, C content, degree of condensation, specific surface area and sorption capacity increased together with pyrolysis temperatures while biochar degradability decreased. The Van Krevelen diagram (Fig. 1) depicts two groups of biochar: one similar to the miscanthus feedstock and one produced above 360 °C closer to lignite, charcoal and anthracite. Increasing pyrolysis temperature decreases the H/C and O/C ratios indicating that the structural transformations induce a carbonization process. Spokas [42] suggested that the O/C molar ratio is the most reliable predictor of the biochar stability. Biochars with O/C ratio comprised between 0.2 and 0.6, as the ones produced at temperatures >360 °C in our study (Fig 1), have been suggested to have a very long half-life (100–1000 years) [42]. More recently Schimmelpfennig & Glaser [43] proposed the combined use of H/C and O/C ratios as a tool to assess the biochar stability with threshold values of $H/C < 0.6$ and $O/C < 0.4$. In the present study miscanthus biochar produced at temperatures >360 °C is under the above-mentioned limit of the O/C ratio but over that of H/C ratio (Fig. 1). Hammes et al. [44] found that a H/C ratio of 0.3 is typical of very highly condensed aromatic ring systems while a H/C of around 0.7, as that of the biochar produced at temperatures >360 °C in the present study, points to a non-condensed aromatic structure such as lignin. The high values of O/C and H/C of biochars produced at 350 and 360 °C suggests low stability and short half-live [43].

4.2. *Thermal analysis*

The DTG profiles of biochars produced at temperatures below 360 °C are similar to that of the original feedstock (Fig. 2). Yang et al. [45] showed that hemicellulose and cellulose start degrading at 220–315 °C and 315–400 °C, respectively. Lignin, on the other hand has a slow degradation with a low mass loss rate over a broader temperature range (100–900 °C). The Miscanthus feedstock and biochars produced at temperatures below 360 °C have one narrow peak (Fig. 2) between 250 and 400 °C, indicating that those degradation reactions are most likely due to the loss of hemicellulose and/or cellulose still present in the biochar structure. The DTG curve of the original feedstock shows a clear shoulder around 270–300 °C, which disappears in the DTG profiles of the biochars (Fig. 2). As reported by other authors [45,46], it is reasonable that this shoulder is caused by the thermal decomposition of hemicellulose. Biochars obtained at temperatures above 360 °C show broader thermal degradation reactions ending at 600 °C due to a series of complex chain reactions characteristic of lignin and lignin-like structures as was confirmed by the O/C ratio around 0.7, which is characteristic of non-condensed aromatic structures [44]. Thermal analysis has confirmed that pyrolysis temperature affects the biochar structure influencing its recalcitrant characteristics.

4.3. *FT-IR spectroscopy*

Thermal analysis results were consistent also with the evolution of FTIR spectra in relation to charring temperature (Fig. 4) which show dehydration and formation of aromatic structures with increasing pyrolysis temperature. Again, the two groups of biochar can be very well distinguished. Low pyrolysis temperatures (<360 °C) biochars behave like the feedstock and maintain a certain hydration and a carbohydrate-like structure. In fact, FTIR spectra still maintain characteristic spectral features of cellulose and hemicellulose (bands between 1200 and 1000 cm^{-1} due to C–O–C and C–O stretchings) [45]. Higher pyrolysis temperatures (>360 °C) cause almost a complete loss of hydration (disappearance of O–H stretching bands at 3500-3200 cm^{-1}) with a concomitant increase in aromaticity [33,47,48]. Aromatic skeletal vibrations (around 1160–1580 cm^{-1} and 1430–1400 cm^{-1}) and aromatic C–H deformation (850–780 cm^{-1}) become in fact dominant in the FTIR spectra of biochars obtained at temperatures >360 °C. In addition, temperatures >360 °C lead to the disappearance of functional groups as carboxyl, carbonyl and hydroxyl groups, i.e. the labile carbon fraction [47,48]. Since biochar might be used as soil amendment these functional groups could play a fundamental role in terms of its contribution to negative sorption sites, which are the main contributors of the cation exchange capacity in soil having thereby a positive impact on nutrient availability and release dynamics.

4.4. *Biochar incubation in soil*

The incubation experiment confirmed a step change in stability between biochars produced at 350–360 °C and those produced at 370–450 °C (Fig. 5b). This finding agrees with that of Zimmerman [23] who found decreasing mineralization rates with increasing charring temperatures, using 6 slow pyrolysis biochars produced from different feedstocks.

Peng et al. [49] incubated for a short period (11 days) slow pyrolysis rice straw biochars produced at temperatures similar to those of our experiment and found a similar mineralization rate pattern that was explained by the removal of the aliphatic structure and the relative increase in aromatic compounds with high pyrolysis temperatures, as was clearly confirmed by the FTIR spectra of the present study (Fig. 4). These results confirm the conceptual model for degradation of fresh biochar [23,50] whereby the biochar would be constituted by two pools: an aliphatic portion that is more readily mineralized and is less abundant in biochar produced at higher temperatures and an aromatic portion that is oxidized more slowly.

5. Conclusions

Thermal analysis coupled with spectroscopic techniques was applied to characterize miscanthus biochar obtained by pyrolysis at different temperatures (350, 360, 370, 400 & 450 °C). Both analytical techniques have shown to be useful tools to assess the chemical and physical characteristics of biochar associated with its stability in soil as confirmed by the mineralization rates measured in the incubation experiment. Stability is a fundamental characteristic for the potential use of biochar both as geoengineering tool for carbon sequestration and agro-technique for enhancing chemical, biological and physical soil fertility. Together with heating rate and feedstock characteristics, pyrolysis temperature has proven to be a fundamental parameter in determining the biochar chemical structure, physical properties and stability. All the analytical techniques agree in identifying a threshold value of pyrolysis temperature at 360 °C, above which the thermal and biological resistance to degradation increased dramatically.

Acknowledgements

The research leading to these results has received funding from the [European Community's] Seventh Framework Programme [FP7/2007-2013] under grant agreement n° 251492. The authors are grateful to Sonja Eichholz, Alex Schindler and Erwin Kaisersberger of Netzsch Gerätebau (Selb, Germany) for their technical assistance.

REFERENCES

[1] Jones A, Panagos P, Barcelo S, Bouraui B, Bosco C, Dewitte O, et al. The state of soil in Europe. A contribution of the JRC to the European environment agency's environment state and outlook report-SOER 2010. Ispar (IT): European Commission Joint Resarch Centre; 2012. p. 78. Report No: EUR 25168 EN.

[2] Laird DA. The charcoal vision: a win-win-win scenario for simultaneously producing bioenergy, permanently sequestering carbon, while improving soil and water quality. Agron J 2008;100(1):178–81.

[3] Sohi S, Lopez-Capel E, Krull E, Bol R. Biochar, climate change and soil: a review to guide future research. Glen Osmond, Australia: CSIRO; 2009 February. p. 64. CSIRO Land and Water Science Report 05/09.
[4] Roberts KG, Gloy BA, Joseph S, Scott NR, Lehmann J. Life cycle assessment of biochar systems: estimating the energetic, economic, and climate change potential. Environ Sci Technol 2010;44(2):827–33.
[5] Galinato SP, Yoder JK, Granatstein D. The economic value of biochar in crop production and carbon sequestration. Energy Policy 2011;39(10):6344–50.
[6] Lewandowski I, Clifton-Brown J, Scurlock J, Huisman W. Miscanthus: European experience with a novel energy crop. Biomass Bioenergy 2000;19(4):209–27.
[7] Brosse N, Dufour A, Meng X, Sun Q, Ragauskas A. Miscanthus: a fast-growing crop for biofuels and chemicals production. Biofuel Bioprod Bior 2012;6(5):580–98.
[8] Heaton E, Long S, Voigt T, Jones M, Clifton-Brown J. Miscanthus for renewable Energy generation: European union experience and projections for illinois. Mitig Adapt Strateg Glob Change 2004;9(4):433–51.
[9] Clifton-Brown JC, Breuer J, Jones MB. Carbon mitigation by the energy crop, Miscanthus. Glob Change Biol 2007;13(11):2296–307.
[10] Hastings A, Clifton-Brown J, Wattenbach M, Mitchell CP, Stampfl P, Smith P. Future energy potential of Miscanthus in Europe. Glob Change Biol Bioenergy 2009;1(2):180–96.
[11] Steiner C, Teixeira WG, Lehmann J, Nehls T, de Macêdo JLV, Blum WEH, et al. Long term effects of manure, charcoal and mineral fertilization on crop production and fertility on a highly weathered central Amazonian upland soil. Plant Soil 2007;291(1–2):275–90.
[12] Sohi SP. Carbon storage with benefits. Science 2012;338(6110):1034–5.
[13] Kwapinski W, Byrne CMP, Kryachko E, Wolfram P, Adley C, Leahy JJ, et al. Biochar from biomass and waste. Waste Biomass Valor 2010;1(2):177–89.
[14] Melligan F, Dussan K, Auccaise R, Novotny EH, Leahy JJ, Hayes MHB, et al. Characterisation of the products from pyrolysis of residues after acid hydrolysis of Miscanthus. Bioresour Technol 2012;108:258–63.
[15] Luo Y, Durenkamp M, De Nobili M, Lin Q, Devonshire BJ, Brookes PC. Microbial biomass growth, following incorporation of biochars produced at 350 °C or 700 °C, in a silty-clay loam soil of high and low pH. Soil Biol Biochem 2013;57:513–23.
[16] Luo Y, Durenkamp M, De Nobili M, Lin Q, Brookes PC. Short term soil priming effects and the mineralisation of biochar following its incorporation to soils of different pH. Soil Biol Biochem 2011;43:2304–14.
[17] Spokas KA, Cantrell KB, Novak JM, Archer DW, Ippolito JA, Collins HP, et al. Biochar: a synthesis of its agronomic impact beyond carbon sequestration. J Environ Qual 2012;41(4):973–89.
[18] Liu X, Zhang A, Ji C, Joseph S, Bian R, Li L, et al. Biochar's effect on crop productivity and the dependence on experimental conditions-a meta-analysis of literature data. Plant Soil. http://dx.doi.org/10.1007/s11104-013-1806-x; 2013.
[19] Clough TJ, Condron LM, Kammann C, Müller C. A review of biochar and soil nitrogen dynamics. Agronomy 2013;3(2):275–93.
[20] DeLuca TH, MacKenzie MD, Gundale MJ. Biochar effects on soil nutrient transformations. In: Lehmann J, Joseph S, editors. Biochar for environmental management: science and technology. London: Earthscan; 2009. pp. 251–70.
[21] Ventura M, Sorrenti G, Panzacchi P, George E, Tonon G. Biochar reduces short-term nitrate leaching from a horizon in an apple orchard. J Environ Qual 2013;42(1):76–82.
[22] Kameyama K, Miyamoto T, Shiono T, Shinogi Y. Influence of sugarcane bagasse-derived biochar application on nitrate leaching in calcaric dark red soil. Environ Sci Technol 2012;41(4):1131–7.
[23] Zimmerman AR. Abiotic and microbial oxidation of laboratory-produced black carbon (biochar). Environ Sci Technol 2010;44(4):1295–301.
[24] Crombie K, Mašek O, Sohi SP, Brownsort P, Cross A. The effect of pyrolysis conditions on biochar stability as determined by three methods. Glob Change Biol Bioenergy 2013;5(2):122–31.
[25] Singh BP, Cowie AL, Smernik RJ. Biochar carbon stability in a clayey soil as a function of feedstock and pyrolysis temperature. Environ Sci Technol 2012;46(21):11770–8.
[26] Gascó G, Paz-Ferreiro J, Méndez A. Thermal analysis of soil amended with sewage sludge and biochar from sewage sludge pyrolysis. J Therm Anal Calorim 2012;108:769–75.
[27] Ameloot N, De Neve S, Jegajeevagan K, Gr Yildiz, Buchan D, Funkuin YN, et al. Short-term CO_2 and N_2O emissions and microbial properties of biochar amended sandy loam soils. Soil Biol Biochem 2013;57(0):401–10.
[28] Downie A, Crosky A, Munroe O. Physical properties of biochar. In: Lehmann J, Joseph S, editors. Biochar for environmental management: science and technology. London: Earthscan; 2009. pp. 13–32.
[29] Alexis M, Rasse DP, Rumpel C, Bardoux G, Péchot N, Schmalzer P, et al. Fire impact on C and N losses and charcoal production in a scrub oak ecosystem. Biogeochemistry 2007;82(2):201–16.
[30] Brewer CE, Unger R, Schmidt-Rohr K, Brown RC. Criteria to select biochars for field studies based on biochar chemical properties. Bioenerg Res 2011;4:312–23.
[31] Masiello CA. New directions in black carbon organic geochemistry. Mar Chem 2004;92(1-4 SPEC. ISS.):201–13.
[32] Baldock JA, Smernik RJ. Chemical composition and bioavailability of thermally altered *Pinus resinosa* (Red pine) wood. Org Geochem 2002;33(9):1093–109.
[33] Kloss S, Zehetner F, Dellantonio A, Hamid R, Ottner F, Liedtke V, et al. Characterization of slow pyrolysis biochars: effects of feedstocks and pyrolysis temperature on biochar properties. J Environ Qual 2012;41(4):990–1000.
[34] Wu W, Yang M, Feng Q, McGrouther K, Wang H, Lu H, et al. Chemical characterization of rice straw-derived biochar for soil amendment. Biomass Bioenergy 2012;47:268–76.
[35] Yang H, Yan R, Chen H, Zheng C, Lee DH, Liang DT. In-depth investigation of biomass pyrolysis based on three major components: hemicellulose, cellulose and lignin. Energy Fuels 2006;20(1):388–93.
[36] Antal MJ, Grønli M. The art, science, and technology of charcoal production. Ind Eng Chem Res 2003;42(8):1619–40.
[37] Ronsse F, van Hecke S, Dickinson D, Prins W. Production and characterization of slow pyrolysis biochar: influence of feedstock type and pyrolysis conditions. Glob Change Biol Bioenergy 2013;5(2):104–15.
[38] Kinney TJ, Masiello CA, Dugan B, Hockaday WC, Dean MR, Zygourakis K, et al. Hydrologic properties of biochars produced at different temperatures. Biomass Bioenergy 2012:4134–43.
[39] Zhang J, You C. Water holding capacity and absorption properties of wood chars. Energy Fuels 2013;27(5):2643–8.
[40] Sun H, Hockaday WC, Masiello CA, Zygourakis K. Multiple controls on the chemical and physical structure of biochars. Ind Eng Chem Res 2012;51(9):3587–97.
[41] Schneider MPW, Hilf M, Vogt UF, Schmidt MWI. The benzene polycarboxylic acid (BPCA) pattern of wood pyrolyzed between 200 °C and 1000 °C. Org Geochem 2010;41(10):1082–8.

[42] Spokas KA. Review of the stability of biochar in soils: predictability of O:C molar ratios. Carbon Manag 2010;1(2):289–303.

[43] Schimmelpfennig S, Glaser B. One step forward toward characterization: some important material properties to distinguish biochars. J Environ Qual 2012;41(4):1001–13.

[44] Hammes K, Smernik RJ, Skjemstad JO, Herzog A, Vogt UF, Schmidt MW. Synthesis and characterisation of laboratory-charred grass straw (*Oryza sativa*) and chestnut wood (*Castanea sativa*) as reference materials for black carbon quantification. Org Geochem 2006;37(11):1629–33.

[45] Yang H, Yan R, Chen H, Lee DH, Zheng C. Characteristics of hemicellulose, cellulose and lignin pyrolysis. Fuel 2007;86(12–13):1781–8.

[46] Sun L, Chen JY, Negulescu JI, Moore MA, Collier BJ. Kinetics modeling of dynamic pyrolysis of bagasse fibers. Bioresour Technol 2011;102:1951–8.

[47] Sharma RK, Wooten JB, Baliga VL, Lin X, Geoffrey Chan W, Hajaligol MR. Characterization of chars from pyrolysis of lignin. Fuel 2004;83(11):1469–82.

[48] Keiluweit M, Nico PS, Johnson MG, Kleber M. Dynamic molecular structure of plant biomass-derived black carbon (biochar). Environ Sci Technol 2010;44(4):1247–53.

[49] Peng X, Ye LL, Wang CH, Zhou H, Sun B. Temperature- and duration-dependent rice straw-derived biochar: characteristics and its effects on soil properties of an Ultisol in southern China. Soil Till Res 2011;112(2):159–66.

[50] Lehmann J, Czimczik C, Laird D, Sohi S. Stability of biochar in soil. In: Lehmann J, Joseph S, editors. Biochar for environmental management. London: Earthscan; 2009. pp. 183–206.

[51] Nikkhah K, Bakhshi NN, MacDonald DG. Co-pyrolysis of various biomass materials and coals in a quartz semi-batch reactor. In: Klass DL, editor. Energy from biomass and wastes XVI. Chicago: Institute of Gas Technology; 1993. pp. 857–902.

[52] van Doorn J, Bruyn P, Vermeij P, Kos B, Hanse J. Combined combustion of biomass, municipal sewage sludge and coal in an atmospheric fluidized bed installation. Petten (NL); ECN 1995. p. 34. Report No.: ECN-C—95-096.

[53] Pentananunt R, Rahman A, Bhattacharya S. Upgrading of biomass by means of torrefaction. Energy 1990;15(12):1175–9.